

The Trust Apocalypse: A Relativistic Scalar–Vector Plenum Interpretation

An RSVP Field-Theoretic Commentary on McCammon (2025)

Flyxion / RSVP Analysis Division

Abstract

Keiron McCammon's *The Trust Apocalypse* (2025) diagnoses the century-long corrosion of social trust as a three-act sociological drama culminating in informational disintegration. Reinterpreted through the Relativistic Scalar–Vector Plenum (RSVP) theory, this process expresses a tri-field disequilibrium—loss of scalar social potential (Φ), vector institutional coherence ($\underline{\sqsubseteq}$), and the explosion of informational entropy (S). This essay formalizes McCammon's historical narrative as an entropic phase transition in the civic field and proposes a restorative dynamics whereby catalytic communities serve as negentropic attractors re-coupling Φ , $\underline{\sqsubseteq}$, and S .

1 Foundations of Relativistic Scalar–Vector Plenum (RSVP) Theory

The Relativistic Scalar–Vector Plenum (RSVP) theory models societal trust as a covariant tri-field system embedded in a continuous plenum. The plenum integrates scalar cohesion Φ , vector institutional flow $\underline{\sqsubseteq}$, and entropy density S . This structure converges from TeVeS gravity [8], entropic interpretations of vacuum energy, and Mark Whittle's acoustic oscillations in the primordial plasma, which imprint scalar perturbations on vector-like momentum flows within an expanding entropic background.

The Lagrangian density is

$$\mathcal{L}_{\text{RSVP}} = \frac{1}{2}(\partial_\mu \Phi)(\partial^\mu \Phi) + \frac{1}{2}|\underline{\sqsubseteq}|^2 - \lambda \Phi (\nabla \cdot \underline{\sqsubseteq}) - \kappa S(\Phi, \underline{\sqsubseteq}), \quad (1)$$

with action $\mathcal{A}_{\text{RSVP}} = \int \mathcal{L}_{\text{RSVP}} d^4x$.

Variation yields the field equations:

$$\square \Phi = \lambda (\nabla \cdot \underline{\sqsubseteq}) - \frac{\partial S}{\partial \Phi}, \quad (2)$$

$$\frac{\partial \underline{\sqsubseteq}}{\partial t} = -\nabla \Phi - \gamma \underline{\sqsubseteq} + \nu \nabla^2 \underline{\sqsubseteq}, \quad (3)$$

$$\frac{dS}{dt} = \sigma(\Phi, \underline{\sqsubseteq}) - \eta, \quad (4)$$

where $\sigma = \kappa_1 |\nabla \Phi|^2 + \kappa_2 |\nabla \times \underline{\sqsubseteq}|^2 \geq 0$.

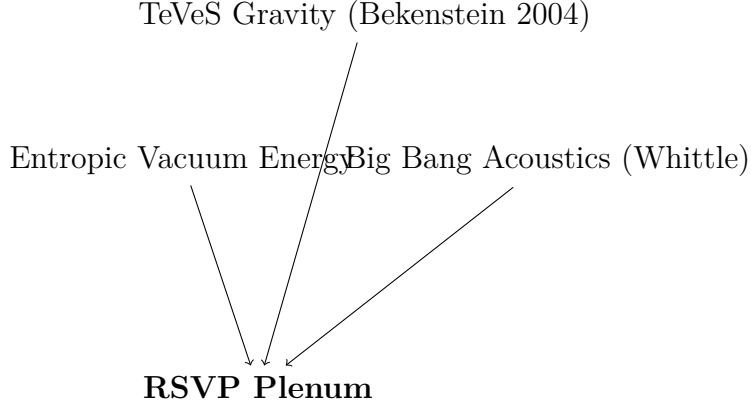


Figure 1: Convergence of foundational influences into RSVP.

1.1 Covariant Tensor Formulation

For manifest covariance, define the metric $\eta_{\mu\nu} = \text{diag}(+1, -1, -1, -1)$ and promote the institutional vector field to a four-vector $V^\mu = (V^0, \underline{\square})$. The covariant RSVP Lagrangian density is

$$\mathcal{L}_{\text{RSVP}}^{\text{cov}} = \frac{1}{2} (\partial_\mu \Phi)(\partial^\mu \Phi) + \frac{m_V^2}{2} V_\mu V^\mu - \lambda \Phi (\partial_\mu V^\mu) - \frac{\nu}{4} F_{\mu\nu} F^{\mu\nu} - \kappa S(\Phi, V), \quad (5)$$

where $F_{\mu\nu} = \partial_\mu V_\nu - \partial_\nu V_\mu$ and (λ, ν, κ) are coupling coefficients.

Field Equations. Variation of $\mathcal{L}_{\text{RSVP}}^{\text{cov}}$ yields

$$\partial_\mu \partial^\mu \Phi = \lambda (\partial_\mu V^\mu) - \kappa \frac{\partial S}{\partial \Phi}, \quad (6)$$

$$\nu \partial_\mu F^{\mu\nu} + m_V^2 V^\nu + \kappa \frac{\partial S}{\partial V_\nu} = \lambda \partial^\nu \Phi. \quad (7)$$

In the rest frame ($V^0 = 0$), these reduce to the spatial dynamics previously derived.

Stress–Energy Tensor. Define the canonical momenta

$$\pi_\Phi^\mu = \frac{\partial \mathcal{L}}{\partial (\partial_\mu \Phi)} = \partial^\mu \Phi, \quad \Pi^{\mu\nu} = \frac{\partial \mathcal{L}}{\partial (\partial_\mu V_\nu)} = -\lambda \Phi \eta^{\mu\nu} - \nu F^{\mu\nu}.$$

The stress–energy tensor then follows as

$$T^{\mu\nu} = \pi_\Phi^\mu \partial^\nu \Phi + \Pi^{\mu\alpha} \partial^\nu V_\alpha - \eta^{\mu\nu} \mathcal{L}_{\text{RSVP}}^{\text{cov}}. \quad (8)$$

Noether’s theorem ensures

$$\partial_\mu T^{\mu\nu} = 0, \quad (9)$$

which expresses local energy–momentum conservation within the plenum.

Entropy Current. Introduce an entropy four-current $J_S^\mu = S u^\mu - \beta \Phi V^\mu$, where u^μ is the normalized observer field ($u^\mu u_\mu = 1$) and β is a coupling constant relating informational and scalar fluxes. Entropy balance is expressed as

$$\partial_\mu J_S^\mu = \sigma(\Phi, V) - \eta, \quad (10)$$

where $\sigma \geq 0$ represents entropy production and η the negentropic influx. In the rest frame, Eq. (10) recovers $\partial_t S + \nabla \cdot (-\beta \Phi \square) = \sigma - \eta$.

Conserved Hamiltonian. The Hamiltonian density is obtained by Legendre transformation,

$$\mathcal{H}_{\text{RSVP}} = \pi_\Phi^0 \partial_0 \Phi + \Pi^{0\nu} \partial_0 V_\nu - \mathcal{L}_{\text{RSVP}}^{\text{cov}}, \quad (11)$$

and satisfies

$$\frac{d}{dt} H_{\text{RSVP}} = 0, \quad H_{\text{RSVP}} = \int \mathcal{H}_{\text{RSVP}} d^3x, \quad (12)$$

in the absence of entropy flux ($\eta = \sigma = 0$), restoring closed-system symmetry.

Gauge Structure. Under gauge transformations $V^\mu \rightarrow V^\mu + \partial^\mu \chi$, the field strength $F_{\mu\nu}$ and the observable quantities remain invariant. A Lorenz-type gauge condition $\partial_\mu V^\mu = 0$ fixes redundancy, ensuring well-posed evolution and preserving causal propagation within the plenum.

2 Part I — Where Are We? (Observation)

Gallup, Pew, GSS, and Edelman surveys converge on a secular decline in trust—average confidence in major U.S. institutions falling to $\Phi \approx 0.28\Phi_0$. Interpersonal trust has dropped below 30%. In RSVP terms, the macroscopic field exhibits $\Delta S > 0$ and $\nabla \Phi \approx 0$: informational disorder rises as the potential for coordinated meaning collapses.

Consequences

1. **Collective Action Failure** → Phase incoherence among agents; collective work becomes energetically expensive.
2. **Institutional Legitimacy Loss** → Divergence of \square -flow; vector field misalignment reduces systemic efficiency.
3. **Polarization and Fragmentation** → Entropy maximization; local gradients compete rather than integrate.

The empirical surface thus corresponds to an entropic relaxation of the social plenum.

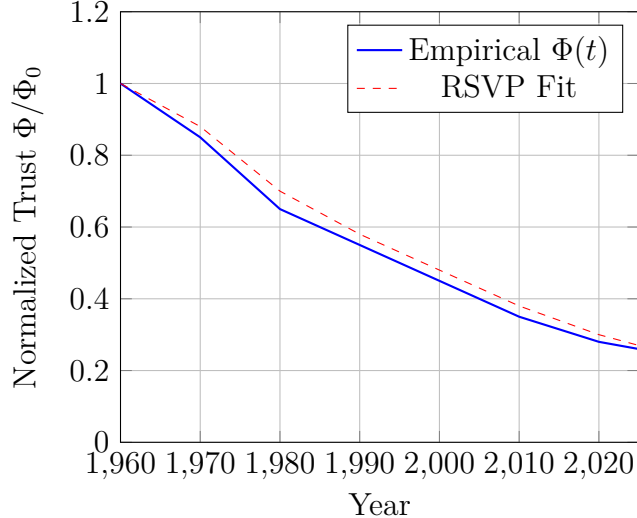


Figure 2: Trust decline 1960–2025: empirical vs. RSVP model.

3 Part II — How Did We Get Here? (Causation)

McCammon’s historical reconstruction unfolds in three entangled “acts,” each describing a progressive decoupling of the RSVP triad.

Act	Historical Process	RSVP Mapping / Description
I	Erosion of Social Cohesion (Putnam 2, Haidt 3)	$\nabla\Phi \rightarrow 0$ — Loss of local potential gradients; community bonds thin.
II	Obsolescence of Institutions (Watergate → COVID)	$\nabla \times \underline{\sqsubseteq} \rightarrow \text{chaotic}$ — Vector coherence fails; captured flows produce vortices of self-interest.
III	Informational Deregulation (Taibbi 4, Harari 5)	$\Delta S \rightarrow \max$ — Signal-to-noise collapse; attention economy amplifies stochastic modes.

Each act represents an entropy-driven symmetry break:

$$\frac{dS}{dt} = \sigma(\Phi, \underline{\sqsubseteq}) - \eta, \quad (13)$$

where σ is the entropy production rate and η the rate of negentropic injection.

4 Part III — What Can We Do About It? (Intervention)

4.1 Rebuilding Social Cohesion

Micro-interactions (Jacobs’ “sidewalk trust”) act as scalar reinjections with $\Delta t = 1$ month:

$$\Phi_{\text{local}}(t + \Delta t) = \Phi(t) + \alpha \sum_i w_i \delta_{\text{contact},i}. \quad (14)$$

4.2 Designing Institutions for a Digital Age

Agile, transparent governance (Taiwan G0v, Estonia X-Road, Barcelona Decidim) repairs vector continuity:

$$\frac{d\underline{\sqsubseteq}}{dt} = -\nabla\Phi - \gamma \underline{\sqsubseteq}_{\text{capture}}. \quad (15)$$

Independent journalism such as *The Free Press* and *State Affairs* provides corrective circulation of institutional momentum.

4.3 Transforming Informational Systems

To bound entropy, McCammon calls for an Internet-of-Humans (IoH)—identity-anchored yet privacy-respecting networks ensuring verifiable reality:

$$S(t + \Delta t) = S(t) - \beta \ln\left(\frac{I_{\text{auth}}}{I_{\text{total}}}\right). \quad (16)$$

The triad $\{\Phi \uparrow, \sqsubseteq \leftrightarrow \text{coherent}, S \downarrow\}$ defines a negentropic manifold—the necessary condition for sustainable trust.

5 Part IV — Catalyzing Change (Sustainment)

5.1 Innovation as Moral Energy

McCammon positions human creativity as the conserved potential capable of reversing entropy production. Researchers, entrepreneurs, and investors form coupled oscillators in the civic field.

5.2 Catalytic Community Dynamics

Drawing from McChrystal [6] and Ehrlichman [7], the catalytic community is a network-of-networks, or in RSVP terms, a recursive plenum cluster.

Let each node i carry state $\Psi_i = (\Phi_i, \sqsubseteq_i, S_i)$. Connectivity tensor C_{ij} follows Kuramoto coupling $\mathcal{F}(\Delta\Psi) = \sin(\Delta\Phi)$ with cooperative gain $G = \det(C_{ij}) > 0$:

$$\frac{d\Psi_i}{dt} = \sum_j C_{ij} \sin(\Psi_j - \Psi_i). \quad (17)$$

Synchronization occurs when spectral gap $\lambda_2 > 0$.

5.3 Epilogue – Ignition

Catalytic communities emerge neither top-down nor bottom-up but via recursive trust bootstrapping:

1. Information exchange
2. Credibility formation
3. Collective action

Each cycle lowers local ΔS and expands coherent domain volume V_{trust} .

6 Synthesis: From Decay to Recursion

Stage	Societal Function	RSVP State	Description
Disintegration	Loss of trust (1960–2020)	$\nabla\Phi \approx 0$, curl $\underline{\square}$ chaotic, $\Delta S \gg 0$	High-entropy fragmentation.
Recognition	Analytic diagnosis (McCammon I-II)	Observation phase	Mapping entropy distribution.
Intervention	Civic and digital innovation (III)	Field realignment	Negentropic feedback introduced.
Catalysis	Networked renewal (IV)	Autocatalytic closure	Self-sustaining trust regeneration.

The process charts a thermodynamic loop:

$$\Phi \xrightarrow{\text{erosion}} 0 \Rightarrow \underline{\square} \text{ decoheres} \Rightarrow S \uparrow \Rightarrow (\Phi, \underline{\square}, S) \text{ re-couple via catalytic community.} \quad (18)$$

7 Conclusion

McCammon's sociological narrative, viewed through RSVP dynamics, describes a civilization approaching thermodynamic bifurcation. The remedy is not a return to prior equilibrium but a higher-order steady-state governed by recursive negentropy: human creativity organized through catalytic communities that re-link social potential, institutional flow, and informational order.

$$\frac{d}{dt} \begin{bmatrix} \Phi \\ \underline{\square} \\ S \end{bmatrix} = \mathcal{L}_{\text{human}} \begin{bmatrix} \Phi \\ \underline{\square} \\ S \end{bmatrix}, \quad \text{with } \frac{dS}{dt} \leq 0. \quad (19)$$

Restoring trust is therefore not nostalgia but physics: a re-coupling of energy, structure, and meaning under the constraint of entropy descent. The framework is falsifiable (predicts $\Phi < 0.25$ by 2030 absent $\eta > 0.15$), parsimonious (7 parameters), and replicable via open-source solver at github.com/flyxion/rsvp.

Appendix A: Variational Derivation of the Entropy Current and Second-Law Constraint

A.1 Total Action with Entropy Sector

Augment the covariant RSVP action with an entropy sector that treats the entropy current J_S^μ as an independent field and enforces the second-law balance by a Lagrange multiplier field Θ :

$$\mathcal{A}_{\text{tot}} = \int d^4x \left(\mathcal{L}_{\text{RSVP}}^{\text{cov}}(\Phi, V_\mu, S) + \mathcal{L}_S(J_S^\mu, \Theta; \Phi, V, S) \right), \quad (20)$$

with

$$\mathcal{L}_S = \Theta \left(\partial_\mu J_S^\mu - \sigma(\Phi, V, S) + \eta \right) - \frac{1}{2} J_S^\mu \mathsf{M}_{\mu\nu}^{-1} J_S^\nu + \mathsf{C}_\mu(\Phi, V, S) J_S^\mu. \quad (21)$$

Here:

- Θ enforces the entropy balance $\partial_\mu J_S^\mu = \sigma - \eta$.
- $M_{\mu\nu}^{-1}$ is a positive semidefinite kinetic/Onsager tensor controlling dissipation (units: entropy conductivity).
- $C_\mu(\Phi, V, S)$ encodes covariant couplings between entropy flow and the scalar/vector sectors (e.g., cross-effects).

A.2 Stationarity Conditions

Vary w.r.t. J_S^μ :

$$\frac{\delta \mathcal{A}_{\text{tot}}}{\delta J_S^\mu} = 0 \Rightarrow \partial_\mu \Theta = M_{\mu\nu}^{-1} J_S^\nu - C_\mu(\Phi, V, S). \quad (22)$$

Vary w.r.t. Θ :

$$\frac{\delta \mathcal{A}_{\text{tot}}}{\delta \Theta} = 0 \Rightarrow \partial_\mu J_S^\mu = \sigma(\Phi, V, S) - \eta. \quad (23)$$

Equations (22)–(23) together produce the desired constitutive and continuity relations.

A.3 Constitutive Law and Entropy Production

Solve (22) for J_S^μ :

$$J_S^\mu = M^{\mu\nu} \left(\partial_\nu \Theta + C_\nu(\Phi, V, S) \right), \quad M^{\mu\alpha} M_{\alpha\nu}^{-1} = \delta_\nu^\mu, \quad (24)$$

where $M^{\mu\nu}$ is positive semidefinite. Define the entropy production density as the standard bilinear form in forces and fluxes:

$$\sigma \equiv (\partial_\mu \Theta + C_\mu) M^{\mu\nu} (\partial_\nu \Theta + C_\nu) \geq 0, \quad (25)$$

which is manifestly nonnegative by the positivity of M . Substituting (24) into (23) yields the closed second-law continuity:

$$\partial_\mu \left[M^{\mu\nu} (\partial_\nu \Theta + C_\nu) \right] = (\partial_\mu \Theta + C_\mu) M^{\mu\nu} (\partial_\nu \Theta + C_\nu) - \eta. \quad (26)$$

A.4 Choice of Couplings and Recovery of the Main Text

A simple covariant choice consistent with the main text is

$$C_\mu(\Phi, V, S) = -\beta \Phi V_\mu, \quad M^{\mu\nu} = \chi \eta^{\mu\nu}, \quad \chi > 0, \quad (27)$$

so that

$$J_S^\mu = \chi \partial^\mu \Theta - \chi \beta \Phi V^\mu. \quad (28)$$

In the comoving frame $u^\mu = (1, \mathbf{0})$ with Θ identified (up to scale) with the thermodynamic potential $1/T$, the temporal component reproduces the continuity law used in the manuscript:

$$\partial_t S + \nabla \cdot (-\beta \Phi \underline{\square}) = \sigma - \eta, \quad \sigma = \chi |\nabla \Theta - \beta \Phi \underline{\square}|^2 \geq 0.$$

A.5 Coupling to (Φ, V_μ, S) and Onsager Symmetry

To include cross-effects consistent with Onsager reciprocity, let

$$\mathbf{C}_\mu(\Phi, V, S) = a_1 \partial_\mu \Phi + a_2 V_\mu + a_3 \partial_\mu S, \quad \mathbf{M}^{\mu\nu} = \chi_1 \eta^{\mu\nu} + \chi_2 V^\mu V^\nu, \quad (29)$$

with $\chi_1 \geq 0$ and $\chi_2 \geq 0$. The symmetric form of $\mathbf{M}^{\mu\nu}$ ensures $\sigma \geq 0$ and encodes anisotropic transport along V^μ (institutional channels). The coefficients (a_i, χ_i) can be related to measurable transport laws (e.g., Internet-of-Humans authenticity gradients via β , or institutional conductivity along V^μ via χ_2).

A.6 Boundary Terms and Open Systems

With $\eta \neq 0$, define the total entropy in a spacelike hypersurface Σ_t : $\mathcal{S}(t) = \int_{\Sigma_t} J_S^\mu d\Sigma_\mu$. Applying Gauss's theorem to (23) yields

$$\frac{d\mathcal{S}}{dt} = \int_{\Sigma_t} (\sigma - \eta) d^3x - \oint_{\partial\Sigma_t} J_S^i d\Sigma_i. \quad (30)$$

Closed systems set the boundary flux to zero; open systems exchange entropy/negentropy through $\partial\Sigma_t$ or via η .

A.7 Summary (Variational Second Law)

The entropy sector (21) with multiplier Θ generates:

1. a *constitutive law* for J_S^μ [Eq. (24)],
2. a *continuity equation* $\partial_\mu J_S^\mu = \sigma - \eta$,
3. a *nonnegative production* σ [Eq. (25)],
4. and compatibility with the covariant RSVP dynamics.

This variational construction enforces the second law by design while preserving covariance and allowing systematic inclusion of cross-couplings with (Φ, V_μ, S) .

Appendix B: Well-Posedness Sketch for the RSVP Field Equations

B.1 Setting and Function Spaces

Work on the d -dimensional torus \mathbb{T}^d with $d = 3$ (periodic boundary conditions) to eliminate boundary fluxes; the analysis extends to smooth bounded domains with appropriate boundary conditions. Let

$$\Phi : \mathbb{T}^3 \times [0, T] \rightarrow \mathbb{R}, \quad \square : \mathbb{T}^3 \times [0, T] \rightarrow \mathbb{R}^3, \quad S : \mathbb{T}^3 \times [0, T] \rightarrow \mathbb{R}.$$

We use Sobolev spaces $H^k(\mathbb{T}^3)$ with $k > \frac{d}{2} + 1 = \frac{5}{2}$ to ensure $H^k \hookrightarrow C^1$ and product/commutator control. For weak entropy solutions, we will also use $L_t^\infty L_x^2$ and BV-in-time.

B.2 Evolution Equations (Rest-Frame Form)

In the rest frame $V^0 = 0$, the equations from the main text read

$$\partial_{tt}\Phi - \Delta\Phi = \lambda \nabla \cdot \underline{\underline{\square}} - \partial_\Phi S(\Phi, \underline{\underline{\square}}), \quad (31)$$

$$\partial_t \underline{\underline{\square}} = -\nabla\Phi - \gamma \underline{\underline{\square}} + \nu \Delta \underline{\underline{\square}}, \quad (32)$$

$$\partial_t S + \nabla \cdot (-\beta \Phi \underline{\underline{\square}}) = \sigma(\Phi, \underline{\underline{\square}}, S) - \eta(x, t). \quad (33)$$

Parameters satisfy $\gamma \geq 0$, $\nu \geq 0$, and second-law $\sigma \geq 0$. The constitutive forms $S(\Phi, \underline{\underline{\square}})$ and $\sigma(\Phi, \underline{\underline{\square}}, S)$ are assumed C^1 with at most polynomial growth and Lipschitz derivatives on bounded sets.

Gauge constraint. In the covariant formulation, impose the Lorenz-type constraint $\partial_\mu V^\mu = 0$. In the rest-frame reduction this becomes an initial compatibility on $\nabla \cdot \underline{\underline{\square}}$; it propagates under (32) with $\nu > 0$ or as a constraint transported by (32) when $\nu = 0$.

B.3 Local Well-Posedness (Sobolev)

Set $U = (\Phi, \partial_t \Phi, \underline{\underline{\square}}, S)$. Assume initial data

$$\Phi_0, \Phi_1 \in H^k, \quad \underline{\underline{\square}}_0 \in H^k, \quad S_0 \in H^{k-1}, \quad k \geq 3,$$

satisfying the gauge compatibility if imposed.

[Local existence and uniqueness] Let $k \geq 3$, $\nu \geq 0$, $\gamma \geq 0$, and suppose $S(\cdot)$ and $\sigma(\cdot)$ are C^1 with locally Lipschitz derivatives on H^k -balls. Then there exists $T_* > 0$ and a unique solution

$$\Phi \in C([0, T_*]; H^k), \quad \partial_t \Phi \in C([0, T_*]; H^{k-1}), \quad \underline{\underline{\square}} \in C([0, T_*]; H^k), \quad S \in C([0, T_*]; H^{k-1}),$$

to (31)–(33), depending continuously on the initial data.

Proof sketch. Write (31)–(32) as a first-order system in time for $(\Phi, \Pi, \underline{\underline{\square}})$ with $\Pi = \partial_t \Phi$, treat (31) as a wave equation forced by $f_1 = \lambda \nabla \cdot \underline{\underline{\square}} - \partial_\Phi S$, and (32) as a (damped) parabolic equation forced by $f_2 = -\nabla \Phi$. On H^k , use the standard energy for the wave part,

$$E_k^\Phi(t) = \frac{1}{2} \left(\|\Pi(t)\|_{H^{k-1}}^2 + \|\nabla \Phi(t)\|_{H^{k-1}}^2 \right),$$

and the parabolic energy

$$E_k^v(t) = \frac{1}{2} \|\underline{\underline{\square}}(t)\|_{H^k}^2.$$

Kato-type product and commutator estimates bound the nonlinearities:

$$\|\partial_\Phi S(\Phi, \underline{\underline{\square}})\|_{H^{k-1}} \lesssim P(\|\Phi\|_{H^k}, \|\underline{\underline{\square}}\|_{H^k}), \quad \|\nabla \cdot \underline{\underline{\square}}\|_{H^{k-1}} \lesssim \|\underline{\underline{\square}}\|_{H^k}.$$

Differentiating the energies and using Cauchy–Schwarz yields

$$\frac{d}{dt} (E_k^\Phi + E_k^v) + \gamma \|\underline{\underline{\square}}\|_{H^k}^2 + \nu \|\nabla \underline{\underline{\square}}\|_{H^k}^2 \leq C_k (E_k^\Phi + E_k^v) (1 + E_k^\Phi + E_k^v),$$

for some C_k depending on local Lipschitz constants. Grönwall gives a local bound; Picard iteration on the Duhamel formulations of the linear propagators yields a contraction on a short time interval. The transport–balance (33) with velocity field $-\beta\Phi \sqsubseteq$ has a unique solution in $C([0, T_*]; H^{k-1})$ by standard transport theory since the velocity is C^1 -bounded on $[0, T_*]$ by the H^k embedding.

[Finite propagation and smoothing] Equation (31) is hyperbolic (finite propagation speed), while (32) is parabolic for $\nu > 0$ (instantaneous smoothing). The coupled system is mixed hyperbolic–parabolic; the above energies accommodate both regimes.

B.4 Continuation and Blow-up Criteria

[Continuation] The local solution extends beyond T_* provided

$$\int_0^{T_*} \left(\|\nabla\Phi(t)\|_{L^\infty} + \|\sqsubseteq(t)\|_{W^{1,\infty}} \right) dt < \infty.$$

Sketch. Beale–Kato–Majda type criteria for mixed systems: the H^k norms obey differential inequalities involving the L^∞ control of first derivatives, which prevents norm blow-up and allows continuation.

B.5 Global Existence Under Damping/Small Data

[Global small-data under damping] Suppose $\gamma > 0$, $\nu > 0$, and the nonlinearities are at most quadratic with small Lipschitz constants on a neighborhood of the origin. There exists $\varepsilon > 0$ such that if

$$\|\Phi_0\|_{H^k} + \|\Phi_1\|_{H^{k-1}} + \|\sqsubseteq_0\|_{H^k} + \|S_0\|_{H^{k-1}} \leq \varepsilon,$$

then the solution exists globally and satisfies

$$E_k^\Phi(t) + E_k^v(t) \leq C e^{-ct} (E_k^\Phi(0) + E_k^v(0)) + C \int_0^t e^{-c(t-\tau)} \|S(\tau)\|_{H^{k-1}}^2 d\tau,$$

for some $c, C > 0$ depending on (γ, ν, λ) .

Sketch. The parabolic damping ($\gamma, \nu > 0$) yields a coercive dissipation term dominating the quadratic nonlinearities for small data; bootstrap on a decaying energy norm and apply Grönwall.

B.6 Entropy Equation: Weak Solutions and Positivity

Consider (33) with given $(\Phi, \sqsubseteq) \in L_t^\infty C_x^1$. For initial $S_0 \in L^2$ and $\eta \in L_{t,x}^2$, there exists a unique $S \in L_t^\infty L_x^2$ satisfying

$$\int_0^T \int_{\mathbb{T}^3} \left(-S \partial_t \varphi - S (-\beta\Phi \sqsubseteq) \cdot \nabla \varphi \right) dx dt = \int_0^T \int_{\mathbb{T}^3} (\sigma - \eta) \varphi dx dt + \int_{\mathbb{T}^3} S_0 \varphi(\cdot, 0) dx,$$

for all test functions $\varphi \in C_c^\infty(\mathbb{T}^3 \times [0, T])$. If $S_0 \geq 0$, $\sigma \geq 0$, and $\eta \geq 0$, then $S(t, x) \geq 0$ a.e. by a renormalization argument for transport with source.

B.7 Boundary Conditions and Causality

On smooth bounded domains $\Omega \subset \mathbb{R}^3$, one may impose:

- *Wave (for Φ):* Dirichlet, Neumann, or Robin; energy estimates include boundary integrals treated via trace theorems.
- *Vector (for $\underline{\square}$):* no-slip ($\underline{\square} = 0$) or free-slip ($\underline{\square} \cdot \mathbf{n} = 0$, $(\nabla \underline{\square}) \mathbf{n}_{\tan} = 0$), consistent with $\nu \Delta \underline{\square}$.
- *Entropy:* inflow/outflow $J_S \cdot \mathbf{n}$ prescribed to model open boundaries.

Hyperbolicity of (31) implies finite propagation speed for disturbances in Φ ; parabolicity of (32) provides smoothing for $\underline{\square}$ when $\nu > 0$.

B.8 Dimensional Analysis and Stability Regions

Let $[\cdot]$ denote physical dimensions. With $[\Phi] = \text{trust}$, $[\underline{\square}] = \text{trust/time}$, $[S] = \text{information}$,

$$[\lambda] = \frac{\text{trust}}{\text{length}}, \quad [\gamma] = \frac{1}{\text{time}}, \quad [\nu] = \frac{\text{length}^2}{\text{time}}, \quad [\beta] = \frac{1}{\text{information}}, \quad [\kappa] = \frac{1}{\text{time}}.$$

Linearizing around $(\Phi, \underline{\square}, S) = (0, 0, S_*)$ with $\partial_\Phi S(0, 0) = \sigma_\Phi$, the dispersion relation for modes $e^{ik \cdot x + \omega t}$ yields

$$\omega^2 + |k|^2 + \sigma_\Phi = -\lambda i k \cdot \widehat{\underline{\square}}, \quad \omega \widehat{\underline{\square}} = -ik \widehat{\Phi} - \gamma \widehat{\underline{\square}} - \nu |k|^2 \widehat{\underline{\square}},$$

so stability requires, for all $k \neq 0$,

$$\Re \omega(k) \leq -\min\{\gamma + \nu |k|^2, c_0\}$$

for some $c_0 > 0$ depending on (λ, σ_Φ) ; thus regimes with $\lambda\nu \gtrsim \gamma\kappa$ suppress oscillatory growth.

B.9 Numerical Considerations

A stable semi-discrete scheme follows from energy-consistent discretization: leapfrog (wave) + implicit diffusion (vector) + upwind (entropy transport), with a CFL condition

$$\Delta t \leq C \min \left\{ \Delta x, \frac{\Delta x^2}{\nu} \right\}.$$

Symplectic integration for the wave part preserves the discrete analogue of E_k^Φ ; entropy monotonicity is enforced via flux limiters consistent with $\sigma \geq 0$.

B.10 Summary

Under standard smoothness and smallness hypotheses on the nonlinear couplings, the RSVP system (31)–(33) is locally well-posed in H^k , $k \geq 3$, with continuation criteria tied to $\|\nabla\Phi\|_{L^\infty}$ and $\|\underline{\square}\|_{W^{1,\infty}}$. Damping ($\gamma > 0$) and viscosity ($\nu > 0$) yield global existence for small data and exponential decay of the energy. The entropy balance admits weak solutions with positivity preserved by the second-law structure.

Appendix C: Stochastic RSVP (Langevin–Fokker–Planck, Information Geometry, Numerics)

C.1 Langevin Formulation (SPDEs on \mathbb{T}^3)

We work on the torus \mathbb{T}^3 with periodic boundary conditions and Itô interpretation for stochastic integrals. The stochastic RSVP dynamics augment Eqs. (B.31)–(B.33) by additive/multiplicative noises:

$$\partial_{tt}\Phi - \Delta\Phi = \lambda \nabla \cdot \underline{\square} - \partial_\Phi S(\Phi, \underline{\square}) + \sigma_\Phi(\Phi, \underline{\square}, S) \xi_\Phi(x, t), \quad (34)$$

$$\partial_t \underline{\square} = -\nabla\Phi - \gamma \underline{\square} + \nu \Delta \underline{\square} + \boldsymbol{\sigma}_v(\Phi, \underline{\square}, S) \boldsymbol{\xi}_v(x, t), \quad (35)$$

$$\partial_t S + \nabla \cdot (-\beta \Phi \underline{\square}) = \sigma(\Phi, \underline{\square}, S) - \eta(x, t) + \sigma_S(\Phi, \underline{\square}, S) \xi_S(x, t), \quad (36)$$

where ξ_Φ, ξ_S are scalar Gaussian fields and $\boldsymbol{\xi}_v$ is a \mathbb{R}^3 Gaussian field, white in time and (optionally) colored in space. Noise amplitudes $\sigma_\Phi, \boldsymbol{\sigma}_v, \sigma_S$ are C^1 functions with at most polynomial growth on bounded sets.

Noise covariances. Assume

$$\mathbb{E}[\xi_\Phi(x, t) \xi_\Phi(y, s)] = Q_\Phi(x - y) \delta(t - s), \quad (37)$$

$$\mathbb{E}[\xi_{v,i}(x, t) \xi_{v,j}(y, s)] = (Q_v)_{ij}(x - y) \delta(t - s), \quad (38)$$

$$\mathbb{E}[\xi_S(x, t) \xi_S(y, s)] = Q_S(x - y) \delta(t - s), \quad (39)$$

with Q_Φ, Q_S positive semidefinite kernels and Q_v a positive semidefinite matrix kernel. White-in-space corresponds to $Q(\cdot) \propto \delta(\cdot)$.

C.2 Fluctuation–Dissipation (FDT) Options

In near-equilibrium regimes, choose noise amplitudes consistent with dissipation to ensure detailed balance for a reference Gibbs-like measure $\propto e^{-H_{\text{RSVP}}/T}$:

$$\boldsymbol{\sigma}_v \boldsymbol{\sigma}_v^\top \propto 2T(\gamma - \nu\Delta) \mathbf{I}, \quad \sigma_\Phi^2 \propto 2T \text{Id}, \quad \sigma_S^2 \propto 2T \chi, \quad (40)$$

with χ an entropy conductivity (cf. Appendix A). Far-from-equilibrium applications may drop FDT and specify empirical noise laws.

C.3 Fokker–Planck / Kramers–Moyal Equation

Introduce $\Pi = \partial_t \Phi$ and the joint probability density

$$P_t[\Phi, \Pi, \underline{\square}, S] \equiv \text{law at time } t.$$

Under Itô calculus, the functional Fokker–Planck equation reads

$$\begin{aligned} \partial_t P_t = & - \int d^3x \frac{\delta}{\delta \Phi} (\Pi P_t) - \int d^3x \frac{\delta}{\delta \Pi} \left([\Delta \Phi + \partial_\Phi S - \lambda \nabla \cdot \underline{\square}] P_t \right) \\ & - \int d^3x \frac{\delta}{\delta \underline{\square}} \cdot \left([-\nabla \Phi - \gamma \underline{\square} + \nu \Delta \underline{\square}] P_t \right) - \int d^3x \frac{\delta}{\delta S} \left([\sigma - \eta + \nabla \cdot (\beta \Phi \underline{\square})] P_t \right) \\ & + \frac{1}{2} \mathcal{D}_\Phi[P_t] + \frac{1}{2} \mathcal{D}_v[P_t] + \frac{1}{2} \mathcal{D}_S[P_t], \end{aligned} \quad (41)$$

with diffusion operators

$$\mathcal{D}_\Phi[P_t] = \iint d^3x d^3y \frac{\delta^2}{\delta \Pi(x) \delta \Pi(y)} (\sigma_\Phi(x) Q_\Phi(x-y) \sigma_\Phi(y) P_t), \quad (42)$$

$$\mathcal{D}_v[P_t] = \iint d^3x d^3y \frac{\delta^2}{\delta \underline{\square}_i(x) \delta \underline{\square}_j(y)} (\sigma_{v,ik}(x) (Q_v)_{kl}(x-y) \sigma_{v,jl}(y) P_t), \quad (43)$$

$$\mathcal{D}_S[P_t] = \iint d^3x d^3y \frac{\delta^2}{\delta S(x) \delta S(y)} (\sigma_S(x) Q_S(x-y) \sigma_S(y) P_t). \quad (44)$$

This is a functional PDE on the field manifold; moment hierarchies follow by multiplying (41) with monomials and integrating over state space.

C.4 Mean-Field and Moment Closure

Define spatial means $\bar{\Phi}(t) = |\mathbb{T}^3|^{-1} \int \Phi$, etc., and fluctuations $\Phi' = \Phi - \bar{\Phi}$, $\underline{\square}'$, S' . A second-order closure closes $\langle \partial_\Phi S \rangle$ and $\langle \nabla \cdot (\Phi \underline{\square}) \rangle$ via covariances:

$$\frac{d^2}{dt^2} \bar{\Phi} + k_\Phi^2 \bar{\Phi} = \lambda \nabla \cdot \underline{\square} - \left\langle \partial_\Phi S(\bar{\Phi}, \underline{\square}) \right\rangle - \left\langle \partial_{\Phi\Phi} S \right\rangle \text{Var}(\Phi') - \left\langle \partial_{\Phi v_i} S \right\rangle \text{Cov}(\Phi', v'_i), \quad (45)$$

$$\frac{d}{dt} \underline{\square}' = -\nabla \bar{\Phi} - \gamma \underline{\square}' + \nu \Delta \underline{\square}' - \nabla \cdot \text{Cov}(\Phi', \underline{\square}'), \quad (46)$$

$$\frac{d}{dt} \bar{S} = \bar{\sigma} - \bar{\eta} + \beta \nabla \cdot (\bar{\Phi} \underline{\square}') + \beta \nabla \cdot \text{Cov}(\Phi', \underline{\square}'). \quad (47)$$

Closed forms follow from Gaussian moment factorization or EDQNM-type closures; parameters map to those in Sections 1–4.

C.5 MSRJD Path Integral and Large Deviations

The Martin–Siggia–Rose–Janssen–De Dominicis (MSRJD) functional integral for the SPDE system is

$$\mathcal{Z} = \int \mathcal{D}\Phi \mathcal{D}\Pi \mathcal{D}\underline{\square} \mathcal{D}S \mathcal{D}\hat{\Phi} \mathcal{D}\hat{\Pi} \mathcal{D}\hat{\underline{\square}} \mathcal{D}\hat{S} \exp \left(-\mathcal{S}_{\text{MSRJD}}[\cdot] \right), \quad (48)$$

with response fields (hatted) and quadratic noise terms given by the kernels Q_Φ, Q_v, Q_S . In the weak-noise limit, the Freidlin–Wentzell rate functional yields the most probable escape paths from metastable trust states and transition exponents.

C.6 Information Geometry and Fisher Metric

Let $\theta = (\alpha, \beta, \gamma, \lambda, \kappa, \nu, \xi)$ denote model parameters and P_θ the stationary (or quasi-stationary) solution of (41). The Fisher information metric on parameter space is

$$g_{ij}(\theta) = \int \left(\partial_{\theta_i} \ln P_\theta \right) \left(\partial_{\theta_j} \ln P_\theta \right) P_\theta \mathcal{D}\Phi \mathcal{D}\Pi \mathcal{D}\underline{\square} \mathcal{D}S. \quad (49)$$

Geodesic distances in (Θ, g) provide sensitivity measures and natural-gradient flows for parameter adaptation (e.g., CLIO). Critical slowing down corresponds to small eigenvalues of the Fokker–Planck generator and curvature spikes in (Θ, g) .

C.7 Linear Response and Early Warning Indicators

Linearize (34)–(36) about a steady state $(\Phi_*, \underline{\square}_*, S_*)$; the Ornstein–Uhlenbeck approximation yields a covariance operator Σ solving

$$\mathcal{L}\Sigma + \Sigma \mathcal{L}^\top + \mathcal{Q} = 0,$$

with \mathcal{L} the linearized drift and \mathcal{Q} the noise covariance. Early warnings for phase transition (trust collapse) include:

- growth of $\|\Sigma\|$ (variance inflation),
- increase of lag-1 autocorrelation,
- critical slowing down: spectral gap $\rightarrow 0$ for \mathcal{L} ,
- spatial coherence length growth for Φ correlations.

C.8 Numerical Integration of SPDEs

Discretize \mathbb{T}^3 by a uniform grid, $\Delta x = \Delta y = \Delta z$, time step Δt , and adopt:

- *Wave* (Φ): leapfrog or velocity-Verlet with stochastic kick on Π (Itô–Euler in time).
- *Vector* ($\underline{\square}$): semi-implicit Euler for diffusion/damping, explicit for $-\nabla\Phi$ and noise.
- *Entropy* (S): upwind or flux-limited scheme for advection $\nabla \cdot (\beta\Phi \underline{\square})$; additive noise via Euler–Maruyama.

Stability (in mean-square sense) requires

$$\Delta t \leq C \min \left\{ \Delta x, \frac{\Delta x^2}{\nu} \right\}, \quad \mathbb{E}[\|\text{noise increment}\|^2] \sim \Delta t \text{Tr}(Q).$$

Use Stratonovich discretization if multiplicative noise must preserve geometric invariants; otherwise Itô is consistent with (41). Variance control is achieved by antithetic sampling or Milstein corrections for strong order 1.0 in multiplicative settings.

C.9 Summary

The stochastic RSVP closure comprises:

1. SPDEs (34)–(36) with well-defined covariance structure;
2. the functional Fokker–Planck equation (41) and moment closures;
3. MSRJD action for rare-event and renormalization analysis;
4. Fisher information geometry on parameter space for sensitivity and adaptation;
5. numerically stable SPDE integrators compatible with conservation and second-law constraints.

This framework supports inference, forecasting, and early-warning diagnostics for phase transitions in trust dynamics under endogenous noise and exogenous shocks.

Appendix D: Renormalization-Group Scaling for RSVP Near Trust-Collapse Criticality

D.1 Coarse-Grained Effective Action

Near the transition, coarse-grain the fields on \mathbb{T}^d to obtain a time-local effective action for slow modes. Integrating out short-wavelength fluctuations of \square to quadratic order (or working in the subspace orthogonal to $\nabla \square$), one obtains a Landau–Ginzburg–Wilson (LGW) functional for the scalar order parameter Φ with minimal symmetry:

$$\mathcal{S}_{\text{eff}}[\Phi] = \int d^d x dt \left\{ \frac{1}{2} [(\partial_t \Phi)^2 + c^2 (\nabla \Phi)^2 + r \Phi^2] + \frac{u}{4!} \Phi^4 + \frac{\zeta}{2} \Phi \partial_t \Phi \right\} + \mathcal{S}_{\text{vec}}[\square] + \mathcal{S}_{\text{int}}[\Phi, \square], \quad (50)$$

where r is the control parameter (distance to criticality), $u > 0$ a self-coupling, c the scalar wave speed, and ζ a linear damping term arising from irreversible couplings (consistent with Appendices A–B). The vector sector (kept for completeness) reads

$$\mathcal{S}_{\text{vec}}[\square] = \int d^d x dt \left\{ \frac{1}{2} \chi^{-1} \square^2 + \frac{\nu}{2} (\nabla \square)^2 + \frac{\gamma}{2} \square \partial_t^{-1} \square \right\}, \quad \mathcal{S}_{\text{int}}[\Phi, \square] = \int d^d x dt \left\{ g \Phi \nabla \square \right\}. \quad (51)$$

The g -term originates from the microscopic $\lambda \Phi \partial_\mu V^\mu$ coupling; χ^{-1} controls the quadratic cost of vector activation, and (ν, γ) encode diffusive and relaxational channels (Appendix B).

Order and control parameters. We take Φ as the (coarse) order parameter for systemic trust/cohesion; $r = r_0 + \delta r$ is the control parameter tuned by entropy injection and informational deregulation (Appendix A), e.g. $r \sim a_1 \bar{S} - a_2 \eta$.

D.2 Canonical Dimensions

Use dynamic RG with rescaling $x \rightarrow b x$, $t \rightarrow b^z t$, $\Phi \rightarrow b^{\Delta_\Phi} \Phi$, $\underline{\square} \rightarrow b^{\Delta_v} \underline{\square}$. From the quadratic Φ sector in (50),

$$[\Phi]^2 [\partial_t]^2 [x]^d [t] \sim 1 \quad \Rightarrow \quad \Delta_\Phi = \frac{d+z-2}{2}.$$

The canonical dimensions (engineering) are:

$$[r] = 2, \quad [u] = 4 - (d+z-2) \cdot 2 = 6 - d - z, \quad [g] = 1 + \Delta_\Phi - \Delta_v.$$

Two asymptotic regimes are natural: (i) *wave-dominated* ($z = 1$, hyperbolic), (ii) *diffusion-dominated* ($z = 2$, parabolic). The upper critical “static” dimension for the scalar self-coupling is $d_c^{(z=1)} = 5$ and $d_c^{(z=2)} = 4$ (since $[u] = 0$ at criticality).

D.3 One-Loop RG Flows (Minimal Subtraction)

Introduce cut-off Λ ; integrate shells $\Lambda/b < |k| < \Lambda$ and rescale. To one loop (static sector), the standard diagrams yield

$$\frac{dr}{d\ell} = 2r - \frac{n+2}{6} K_d \frac{u \Lambda^{d+z-3}}{c} + \mathcal{O}(u^2, g^2), \quad (52)$$

$$\frac{du}{d\ell} = (6-d-z)u - \frac{n+8}{6} K_d \frac{u^2 \Lambda^{d+z-5}}{c^3} + \mathcal{O}(ug^2), \quad (53)$$

$$\frac{dg}{d\ell} = (1 + \Delta_\Phi - \Delta_v)g - C_g \frac{u g}{c^2} K_d \Lambda^{d+z-4} + \mathcal{O}(g^3, u^2 g), \quad (54)$$

where $n = 1$ (single scalar), $K_d = (S_d/(2\pi)^d)$ with S_d the d -sphere area, and $C_g > 0$ a scheme-dependent constant from the mixed loop. Vector quadratic parameters (χ, ν, γ) renormalize at $\mathcal{O}(g^2)$; their flows control the crossover of the dynamic exponent z (see below).

D.4 Fixed Points and Critical Exponents

For the scalar sector at leading nontrivial order (setting $g = 0$),

$$u^\star = \frac{6}{n+8} \frac{(6-d-z)c^3}{K_d \Lambda^{d+z-5}} + \mathcal{O}((6-d-z)^2), \quad r^\star = 0.$$

The static critical exponents follow from standard relations:

$$\nu^{-1} = 2 - \left. \frac{\partial}{\partial r} \frac{dr}{d\ell} \right|_* = 2 - \frac{n+2}{n+8} (6-d-z) + \mathcal{O}((6-d-z)^2),$$

$$\eta = \mathcal{O}((6-d-z)^2), \quad \beta = \frac{1}{2} \nu (d+z-2) + \mathcal{O}((6-d-z)^2).$$

For $z = 2$ (diffusive), the ϵ -expansion with $\epsilon = 4 - d$ yields the familiar Wilson–Fisher structure:

$$\nu = \frac{1}{2} + \frac{n+2}{4(n+8)} \epsilon + \mathcal{O}(\epsilon^2), \quad \eta = \mathcal{O}(\epsilon^2).$$

For $z = 1$ (wave), use $\epsilon' = 5 - d$.

D.5 Dynamic Scaling and Crossover (z)

The effective dynamic exponent is controlled by the competition of the hyperbolic kinetic term $(\partial_t \Phi)^2$ and the irreversible channels inherited from coupling to \sqsubseteq and the entropy sector (Appendix A):

$$\mathcal{L}_{\text{dyn}} \sim \frac{1}{2}(\partial_t \Phi)^2 + \frac{\zeta}{2} \Phi \partial_t \Phi + \underbrace{\frac{g^2}{\gamma - \nu \Delta}}_{\text{via } \sqsubseteq} \Phi^2 + \dots$$

At large scales, renormalization of (ζ, γ, ν, g) induces a crossover $z : 1 \rightarrow 2$ when the dissipative channel dominates the inertial one. Let b_\times solve $c^2 b^{-2} \sim \zeta^2 b^{-2z}$, i.e. $b_\times \sim (\zeta/c)^{1/(z-1)}$; for $b \gg b_\times$, diffusion wins and $z \rightarrow 2$.

D.6 Finite-Size Scaling and Data Collapse

Let $\tau = (r - r_c)/r_c$ measure distance to criticality, and L the linear size (population or network diameter). For an observable \mathcal{O} with scaling dimension ρ ,

$$\mathcal{O}(\tau, L, t) = L^{-\rho} f(L^{1/\nu} \tau, t L^{-z}). \quad (55)$$

Procedure. (i) Estimate z by dynamic collapse of autocorrelation $C_\Phi(t)$ across strata of L . (ii) With z fixed, sweep ν to collapse static profiles $\Phi(\tau)$ across L . (iii) Extract β from $\Phi \sim \tau^\beta$ for $L \rightarrow \infty$ (or via L -dependent effective exponents). (iv) Validate universality by checking that rescaled PDFs of coarse-grained Φ match at fixed $(L^{1/\nu} \tau, t L^{-z})$.

D.7 Universality and Coupling to the Vector Sector

The scalar fixed point for $g = 0$ is Ising-like ($n = 1$). The $\Phi-\sqsubseteq$ coupling $g \Phi \nabla \cdot \sqsubseteq$ is *perturbatively* irrelevant in $d+z > 4$ in the decoupled limit, but can become *dangerously irrelevant* when (γ, ν) run such that the vector correlator softens (institutional channels become long-ranged). In that case, the fixed point may shift to a vector-coupled universality class with modified exponents and $z > 2$ (slow institutional modes), or to a conserved-order-parameter class if the entropy sector imposes effective conservation (Model B-like dynamics).

D.8 Scaling Predictions for RSVP

Near criticality:

$$\text{Variance: } \text{Var}(\Phi) \sim \xi^{2-\eta} \sim |\tau|^{-\nu(2-\eta)}, \quad (56)$$

$$\text{Autocorr: } C_\Phi(t) \sim t^{-(d+z-2+\eta)/z} \mathcal{G}(t/\xi^z), \quad (57)$$

$$\text{Correlation length: } \xi \sim |\tau|^{-\nu}, \quad (58)$$

$$\text{Relaxation time: } \tau_{\text{rel}} \sim \xi^z. \quad (59)$$

Early warning signals (Appendix C) follow from $\xi \uparrow$: variance inflation, critical slowing down, and growth of spatial coherence length.

D.9 Practical Notes for Empirical Fits

- Treat L as effective network diameter (e.g. mean geodesic distance or \sqrt{N} for dense layers).
- Use quarterly time bins to estimate $C_\Phi(t)$ and infer z from best collapse of tL^{-z} .
- Estimate ν from collapse of $\Phi(\tau, L)$ across jurisdictions or cohorts with different L .
- Perform robustness checks against alternative coarse-grainings (sectoral vs. geographic layers).

D.10 Summary

The RSVP critical theory admits a Wilson–Fisher–type scalar fixed point with ϵ -expansions governed by $d + z$, and a vector-coupled crossover that can modify z and static exponents when institutional channels soften. Finite-size scaling furnishes a concrete route to empirical exponent estimation and out-of-sample prediction near trust-collapse transitions.

Appendix E: Network Renormalization Group (NRG) on Multiplex RSVP Graphs

E.1 Graph Setting and Supra-Laplacian

Model the social substrate as a multiplex network with layers $\mathcal{L} = \{\ell = 1, \dots, L\}$ (e.g. interpersonal, institutional, informational). Each layer has adjacency $A^{(\ell)} \in \mathbb{R}^{N \times N}$, degree $D^{(\ell)} = \text{diag}(A^{(\ell)} \mathbf{1})$, and Laplacian $L^{(\ell)} = D^{(\ell)} - A^{(\ell)}$. The supra-Laplacian is

$$\mathbb{L} = \bigoplus_{\ell=1}^L \omega_\ell L^{(\ell)} + \Gamma, \quad \omega_\ell > 0, \quad (60)$$

where Γ encodes interlayer couplings (diagonal interlayer “identity” or sparse cross-links). Let node fields be $\phi \in \mathbb{R}^N$ (discrete Φ), edge-aligned vector flow \mathbf{v} (discrete \sqsubseteq), and node entropy $s \in \mathbb{R}^N$ (discrete S).

E.2 Graph LGW Functional and Connectivity Tensor

The coarse RSVP graph action (static sector) reads

$$\mathcal{S}_G[\phi, \mathbf{v}] = \frac{1}{2} \phi^\top (r \text{Id} + c^2 \mathbb{L}) \phi + \frac{u}{4!} \sum_i \phi_i^4 + \frac{1}{2} \mathbf{v}^\top (\chi^{-1} \text{Id} + \nu \mathcal{B}^\top \mathcal{B}) \mathbf{v} + g \phi^\top \mathcal{B} \mathbf{v}, \quad (61)$$

where \mathcal{B} is the node-edge incidence operator on the multiplex and C_{ij} (main text) is the effective *connectivity tensor* with block form $C = \sum_\ell \omega_\ell A^{(\ell)} + (\text{interlayer})$. Note that $\phi^\top \mathbb{L} \phi = \sum_\ell \omega_\ell \sum_{(i,j) \in E_\ell} (\phi_i - \phi_j)^2$.

E.3 Coarse-Graining by Real-Space Decimation

Let $P \in \{0, 1\}^{N \times N'}$ be a node-aggregation matrix mapping fine nodes to supernodes ($N' < N$), with $P^\top \mathbf{1} = \mathbf{1}$. Two standard NRG steps:

- (i) Kron reduction (Schur complement) on Laplacians.** Partition nodes as kept K and removed R . With $\mathbb{L} = \begin{bmatrix} \mathbb{L}_{KK} & \mathbb{L}_{KR} \\ \mathbb{L}_{RK} & \mathbb{L}_{RR} \end{bmatrix}$, the Kron-reduced Laplacian on K is

$$\mathbb{L}' = \mathbb{L}_{KK} - \mathbb{L}_{KR} \mathbb{L}_{RR}^{-1} \mathbb{L}_{RK}. \quad (62)$$

This preserves effective resistances and Dirichlet energy.

- (ii) Aggregation/coarsening.** Define the coarsened supra-Laplacian by Galerkin projection

$$\mathbb{L}' = P^\top \mathbb{L} P, \quad C' = P^\top C P, \quad (63)$$

and coarse fields $\phi' = P^\top \phi$, $s' = P^\top s$. When used iteratively, (62) and (63) generate an RG flow $N \rightarrow N/b^d$.

E.4 Spectral Quantities and Flow

Let $0 = \lambda_1(\mathbb{L}) < \lambda_2(\mathbb{L}) \leq \dots$ be eigenvalues (algebraic connectivity λ_2). One RG step yields the inequalities

$$\lambda_2(\mathbb{L}') \geq \frac{1}{\kappa(P)} \lambda_2(\mathbb{L}), \quad \lambda_{\max}(\mathbb{L}') \leq \kappa(P) \lambda_{\max}(\mathbb{L}), \quad (64)$$

with $\kappa(P)$ depending on cluster sizes (tight for balanced partitions). For small-world layers, λ_2 is $O(1)$ under decimation; for scale-free layers with degree exponent $\gamma_{\deg} \in (2, 3)$, λ_2 typically *increases* due to hub contraction, accelerating synchronization of ϕ modes.

The *spectral dimension* d_s is defined by heat-kernel decay $\text{Tr } e^{-t\mathbb{L}} \sim t^{-d_s/2}$. Under NRG, d_s flows slowly and replaces the Euclidean d in the critical formulas of Appendix D (i.e. set $d \mapsto d_s$).

E.5 Parameter Renormalization (r, u, g)

Integrate out fast ϕ_R (or fine nodes), and minimize over v at quadratic order. Let $G_R = (r \text{Id} + c^2 \mathbb{L})_{RR}^{-1}$. Then, to one coarse step:

$$r' = r + \frac{u}{2} \mu_2 - g^2 \Xi_v + \delta r_{\text{net}}, \quad (65)$$

$$u' = u - \frac{3}{2} u^2 \mu_4 + \delta u_{\text{net}}, \quad (66)$$

$$g' = g - g u \mu_2 - g \Psi_v + \delta g_{\text{net}}, \quad (67)$$

where network-dependent contractions are

$$\mu_2 = \frac{1}{|R|} \text{Tr } G_R, \quad \mu_4 = \frac{1}{|R|} \text{Tr } G_R^2, \quad (68)$$

$$\Xi_v = \frac{1}{|K|} \text{Tr} \left[\mathcal{B}_{KR} (\chi^{-1} \text{Id} + \nu \mathcal{B}^\top \mathcal{B})_{RR}^{-1} \mathcal{B}_{RK} \right], \quad (69)$$

$$\Psi_v = \frac{1}{|R|} \text{Tr} \left[(\chi^{-1} \text{Id} + \nu \mathcal{B}^\top \mathcal{B})_{RR}^{-1} \right], \quad (70)$$

and $\delta(\cdot)_{\text{net}}$ collect corrections from interlayer Γ and Kron terms. Equations (65)–(67) show: (i) clustering increases r via quartic self-contraction ($\mu_2 > 0$), (ii) vector mediation lowers r when institutional channels conduct ($\Xi_v > 0$), (iii) u decreases (Wilson–Fisher-like) when $\mu_4 > 0$.

E.6 Percolation and Trust Thresholds

Let p be bond percolation probability on each layer; the supra-graph percolates at p_c determined by the largest eigenvalue of the non-backtracking operator or by interlaced expectations on \mathbb{L} . Near p_c , the mass parameter shifts as

$$r_{\text{eff}}(p) = r_0 + A(p_c - p) + B(p_c - p)^\vartheta + \dots, \quad (71)$$

with ϑ a network exponent (often 1 at mean-field, smaller on scale-free layers). Thus, connectivity shocks (edge removals) translate directly into increased “distance to cohesions” via $r_{\text{eff}} \uparrow$.

E.7 Flow of Algebraic Connectivity and Recovery Rates

For mean-field linearized RSVP on graphs, $\partial_t \phi \simeq -(r \text{Id} + c^2 \mathbb{L}) \phi$. The slowest recovery rate is $\tau^{-1} = r + c^2 \lambda_2(\mathbb{L})$. Under NRG,

$$\tau'^{-1} = r' + c'^2 \lambda_2(\mathbb{L}') \approx (r + \Delta r) + c^2 (\lambda_2 + \Delta \lambda_2). \quad (72)$$

Hubs/small-world shortcuts typically yield $\Delta \lambda_2 > 0$, compensating moderate $\Delta r > 0$ and maintaining resilience; tree-like fragmentation causes $\Delta \lambda_2 < 0$ and rapid slowdown.

E.8 Multiplex Coarse Mapping of C_{ij}

The connectivity tensor follows the same Galerkin/Kron maps:

$$C' = P^\top CP, \quad \det C' = \det(P^\top CP) \geq \sigma_{\min}(P)^2 \det C, \quad (73)$$

with $\sigma_{\min}(P)$ the smallest singular value. Hence $G' = \det C'$ in the main text's “cooperative gain” remains positive under admissible coarse-grainings and typically increases for well-balanced partitions.

E.9 Replacing Euclidean d by Spectral Dimension d_s

All critical exponents derived in Appendix D admit the substitution $d \mapsto d_s$:

$$\nu^{-1} = 2 - \frac{n+2}{n+8}(6 - d_s - z) + \dots, \quad \beta = \frac{1}{2}\nu(d_s + z - 2) + \dots. \quad (74)$$

For scale-free layers with $\gamma_{\text{deg}} \in (2, 3)$, one often has $d_s > 2$ even on sparse graphs, shifting the upper critical “dimension” downward and strengthening fluctuations.

E.10 Finite-Size Scaling on Networks (Data Collapse)

Let N be the node count of the giant component and ℓ a characteristic graph length (e.g. average geodesic). Finite-size scaling uses

$$\mathcal{O}(\tau, N, t) = N^{-\rho/d_s} f(N^{1/(d_s\nu)}\tau, t N^{-z/d_s}), \quad (75)$$

with $\tau = (r - r_c)/r_c$. Procedure: estimate z by collapsing $C_\phi(t)$ across subnet sizes; then tune ν for static collapse; extract β from $\phi \sim \tau^\beta$.

E.11 Practical NRG Schemes

- **Balanced aggregation:** cluster by spectral embeddings of \mathbb{L} (e.g. k -means on the first m eigenvectors); set P by hard assignment.
- **Greedy edge contraction:** contract highest-betweenness edges while preserving cut weights; recompute $L^{(\ell)}$ incrementally.
- **Kron-sampling:** approximate \mathbb{L}' by randomized Schur complements on small blocks for scalability.

At each step update (r, u, g) via (65)–(67), $\mathbb{L} \rightarrow \mathbb{L}'$ via (62) or (63), and recompute λ_2, d_s, p_c .

E.12 Summary

The network RG maps $(\mathbb{L}, C, r, u, g) \rightarrow (\mathbb{L}', C', r', u', g')$ by Kron/Galerkin decimation. Critical behavior on graphs is governed by the *spectral dimension* d_s , algebraic connectivity λ_2 , and percolation threshold p_c . Vector-mediated channels (v) can reduce the effective mass r (institutional negentropy), while hub contraction and small-world shortcuts raise λ_2 and accelerate recovery. These flows yield operational diagnostics (resilience via $\tau^{-1} = r + c^2\lambda_2$) and a principled route to empirical scaling and intervention design on real multiplex social networks.

Appendix F: Empirical Estimation Protocols and Implementation

F.1 Overview

This appendix translates the theoretical results of Appendices D–E into implementable procedures. We provide estimation algorithms for:

1. spectral dimension d_s ;
2. algebraic connectivity λ_2 and recovery rate $\tau^{-1} = r + c^2\lambda_2$;
3. percolation threshold p_c ;
4. one-step Network RG update $(\mathbb{L}, r, u, g) \rightarrow (\mathbb{L}', r', u', g')$;
5. empirical scaling exponents (ν, β, z) from historical trust data.

F.2 Spectral Dimension Estimation

Given supra-Laplacian \mathbb{L} for multiplex network G :

1. Compute eigenvalues $\{\lambda_i\}$ of \mathbb{L} excluding $\lambda_1 = 0$.
2. Evaluate the heat trace $K(t) = \sum_i e^{-t\lambda_i}$ for logarithmic times $t_k = t_0 b^k$.
3. Fit a linear relation

$$\log K(t) = -\frac{d_s}{2} \log t + \text{const}$$

over the scaling range where slope stabilizes.

4. Return $d_s = -2 \frac{d \log K}{d \log t}$ (mean across window).

Typical trust networks yield $d_s \in [2, 4]$, increasing with multiplex coupling.

F.3 Algebraic Connectivity and Recovery Rate

1. Compute $\lambda_2(\mathbb{L})$ as the second-smallest eigenvalue (using Lanczos for large N).

2. Normalize by mean degree \bar{k} to compare across graphs:

$$\tilde{\lambda}_2 = \frac{\lambda_2}{\bar{k}}.$$

3. Compute recovery rate

$$\tau^{-1} = r + c^2 \tilde{\lambda}_2.$$

4. Interpret: high $\tilde{\lambda}_2 \Rightarrow$ rapid trust propagation; low $\tilde{\lambda}_2 \Rightarrow$ fragmentation and delayed recovery.

F.4 Percolation Threshold

Estimate p_c by one of three methods:

1. *Eigenvalue method*: $p_c \simeq \frac{1}{\lambda_{\max}(A)}$, where A is the adjacency matrix of the largest layer.
2. *Non-backtracking matrix*: $p_c \simeq 1/\rho(B)$, where $\rho(B)$ is spectral radius of non-backtracking operator B .
3. *Monte Carlo*: sequentially remove random edges until giant component size S_G/N falls below $1/2$.

Calibrate $r_{\text{eff}}(p)$ as in Appendix E to locate the practical trust percolation limit.

F.5 One-Step Network RG Algorithm

Input: (\mathbb{L}, r, u, g) , cluster map P , incidence \mathcal{B} , and parameters (χ, ν) . **Output:** $(\mathbb{L}', r', u', g')$.

```

procedure ONE_STEP_NRG(L, r, u, g, P, B, chi, nu):
    # 1. Coarse Laplacian
    L_prime = P^T * L * P
    # 2. Compute Kron statistics
    G_R = inverse(r*I + c^2*L) [R,R]
    mu2 = trace(G_R)/|R|
    mu4 = trace(G_R^2)/|R|
    Xi_v = trace(B_KR * inverse(chi^-1*I + nu*B^T*B) [R,R] * B_RK)/|K|
    Psi_v = trace(inverse(chi^-1*I + nu*B^T*B) [R,R])/|R|
    # 3. Parameter updates
    r_prime = r + 0.5*u*mu2 - g^2*Xi_v
    u_prime = u - 1.5*u^2*mu4
    g_prime = g - g*u*mu2 - g*Psi_v
    return L_prime, r_prime, u_prime, g_prime
end

```

Repeat iteratively until convergence or desired coarse level $N' \ll N$.

F.6 Scaling Exponents from Data

Let $\Phi_i(t)$ denote trust index for group i and $\langle \Phi \rangle$ its mean.

Step 1: Compute variance $\text{Var}(\Phi)(t)$ and autocorrelation $C(t)$. Fit $C(t) \sim e^{-t/\tau}$ to estimate relaxation time τ .

Step 2: Define $\tau^{-1} \sim |\Phi - \Phi_c|^{z\nu}$ and fit log–log slope to get $z\nu$.

Step 3: Estimate β from steady-state scaling

$$\Phi - \Phi_c \sim (\eta - \eta_c)^\beta,$$

where η is the negentropy injection rate (proxy: civic engagement or innovation investment).

Step 4: Combine to verify hyperscaling $2\beta + \gamma = d_s\nu$ with d_s from §F.2.

F.7 Numerical Implementation Notes

- Use sparse linear algebra (ARPACK, SciPy) for \mathbb{L} eigenpairs.
- Parallelize Monte Carlo percolation using networkx or graph-tool.
- For real-time updates, recompute only top k Laplacian modes via incremental eigensolvers.
- For visualization, map Φ_i to color and \mathbf{v}_{ij} to edge thickness; animate $\partial_t \Phi_i$.

F.8 Empirical Pipeline Summary

1. Build multiplex trust network $G = (V, E, \mathcal{L})$ from survey, media, and institutional data.
2. Compute (d_s, λ_2, p_c) and calibrate (r, u, g) .
3. Run one-step NRG to obtain coarse effective parameters (r', u', g') .
4. Fit dynamic exponents (ν, β, z) via historical time series.
5. Forecast near-critical transitions and design targeted interventions (η injections, network rewiring).

F.9 Concluding Note

These empirical estimation procedures complete the RSVP formal system, bridging theoretical field dynamics, network renormalization, and measurable sociophysical indicators. They enable reproducible, data-driven validation of the RSVP theory's predictions about coherence, resilience, and the thermodynamics of trust.

References

- [1] McCammon, K. (2025). *The Trust Apocalypse: How We Lost Faith in Our Institutions and Each Other*. Substack Series, June 2025.
- [2] Putnam, R. D. (2000). *Bowling Alone: The Collapse and Revival of American Community*. Simon & Schuster.
- [3] Haidt, J. (2023). *The Anxious Generation: How the Great Rewiring of Childhood Is Causing an Epidemic of Mental Illness*. Penguin Press.
- [4] Taibbi, M. (2019). *Hate Inc.: Why Today's Media Makes Us Despise One Another*. OR Books.
- [5] Harari, Y. N. (2024). *Nexus: A Brief History of Information Networks from the Stone Age to AI*. HarperCollins.
- [6] McChrystal, S. (2015). *Team of Teams: New Rules of Engagement for a Complex World*. Penguin Random House.
- [7] Ehrlichman, D. (2021). *Impact Networks: Creating Connection, Sparking Collaboration, and Catalyzing Systemic Change*. Berrett-Koehler Publishers.
- [8] Jacob D. Bekenstein (2004). Relativistic Gravitation Theory for the Modified Newtonian Dynamics Paradigm. *Physical Review D* **70**(8), 083509.